Formation and transition of labyrinthine domain patterns in a nonlinear optical system

Weiping Lu* and Svetlana L. Lachinova†
Department of Physics, Heriot-Watt University, Edinburgh, EH14 4AS, United Kingdom
(Received 15 May 2000; revised manuscript received 19 July 2000; published 11 December 2000)

We report numerical and theoretical investigations of the formation and transition of domain patterns in a two-dimensional optical system with cosine-type nonlinearity and a feedback loop. Labyrinthine stripe domain patterns of the electric field are observed in the system, intiated from the Turing instability. The labyrinths are found to undergo a transition to domain patterns of coexisting stripes and hexagons and disordered hexagon domains on variation of the incident field intensity, a control parameter of the system. The parameter regions for these domain structures are explained through the existence and competition of stripes and hexagons in terms of their amplitude equations. Moreover, the transition from straight stripes to labyrinths is investigated by varying the feedback coupling coefficient of the system. The transition is shown to be the consequence of coexistence of and interaction between stripes and domain walls.

DOI: 10.1103/PhysRevA.63.013807 PACS number(s): 42.65.Sf

Labyrinthine patterns are nonequilibrium spatial structures that take the form of a mosaic of striped patches in spatially extended systems, each of which has a fixed but arbitrary orientation and almost constant wavelength. Labyrinths were first observed experimentally from a sequence of transverse smectic instabilities culminating in the generation of disclination dipoles in ferrimagnetic material [1–3]. Such patterns have been studied in various theoretical models such as distributed oscillators [4] and Rayleigh-Bénard convection [5] as spontaneous pattern formation and in reaction-diffusion systems as excitable spatial structures [6]. The fact that virtually the same patterns occur in physically diverse systems has motivated a mathematical framework that considers common symmetries of these systems, general principles for their underlying formation, and descriptions of their macroscopic structure. In recent work a simplified mathematical model, the linear Helmholtz equation, was derived from reduction of the fourth-order nonlinear diffusion equation to provide a better understanding of the nature of the disordered roll patterns [7]. Moreover, wavelet transform has been used as a tool linking data provided from experiments and computer simulations to the macroscopic order parameters obtained from theory [8], thus offering important means for comparison of experiment with theory. In this article, we investigate the formation of labyrinthine domain patterns in a two-dimensional optical system with cosine-type nonlinearity and a feedback loop. Disordered stripe domain patterns in both phase and amplitude of the electric field are observed numerically in the system, arising initially from the Turing instability. The labyrinths are found to undergo a transition to domain patterns of coexisting stripes and hexagons and then to disordered hexagon domains on variation of the control parameters of the incident field intensity in the system. The parameter regions for these domain structures are explained through the existence and competition of stripes and hexagons in terms of their amplitude equations. Moreover, the coarsening process describing the transition between straight stripes and labyrinthine domain patterns is investigated on varying the feedback coupling coefficient of the system. The coexistence and interaction of stripes and domain walls is found to be attributable to labyrinth formation in this system.

Our model comprises a spatially extended two-dimensional light-phase modulator of reflection type coupled with a feedback loop, the schematic being shown in Fig. 1(a) [9]. The nonlinearity of the phase modulator, i.e., the functional dependence of the phase modulation on the incident field intensity, is chosen to be cosine type. Such a nonlinear ''medium'' can be electronically synthesized in actual experiments using optoelectronic feedback as demonstrated recently in Ref. [10]. The hybrid optoelectronic approach showed flexible selection and control in operation of the nonlinear system and different optical pattern formations, such as web structures and black eyes, were observed using bimodal, unimodal, and piecewise nonlinearities in such a system [10].

The dynamics of phase variation $u(\mathbf{r},t)$ of a propagating light wave in a thin nonlinear medium is described by the diffusive equation

$$\tau_0 \frac{\partial u(\mathbf{r},t)}{\partial t} + u(\mathbf{r},t) = D\nabla_\perp^2 u(\mathbf{r},t) + K\{1-\cos[2\pi I_d(\mathbf{r},t)]\}, \tag{1}$$

where $\mathbf{r}$ is the radius vector in the transverse plane, t the time coordinate, and τ_0 the characteristic relaxation time of the

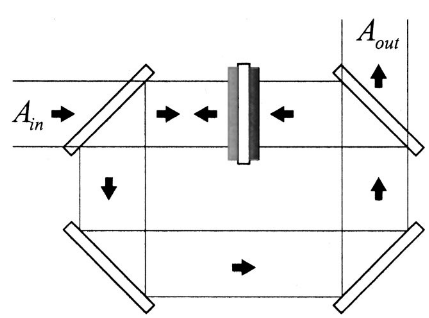

FIG. 1. Schematic of the nonlinear optical system with feedback. $A_{\rm in}$ and $A_{\rm out}$ are the complex amplitudes of input and output fields, respectively.

*Email address: phywl@phy.hw.ac.uk
†Email address: physl.phy.hw@phyfsa.phy.hw.ac.uk

nonlinearity. D is the diffusion coefficient related to the diffusion length of the nonlinear medium, $\nabla_\perp^2$ the transverse Laplacian, and K the feedback coupling coefficient. $I_d(\mathbf{r},t)=|A(\mathbf{r},z=L,t)|^2$ is the intensity distribution of the light wave A registered on the other side of the phase modulator, after propagation in the feedback loop of length L. The last is described by the free-space propagation equation in the paraxial approximation,

$$-2ik_0\frac{\partial A(\mathbf{r},z,t)}{\partial z}=\nabla_\perp^2 A(\mathbf{r},z,t) \tag{2}$$

with the range in the longitudinal direction $0\leqslant z\leqslant L$ and the boundary condition

$$A(\mathbf{r},z=0,t)=A_0\exp[iu(\mathbf{r},t)], \tag{3}$$

where $k_0=2\pi/\lambda$ is the wave number. $A_0=R\sqrt{1-R}A_{\mathrm{in}}$ is the effective incident field amplitude registered on the front face of the phase modulator, where A_{in} is the input field amplitude outside the cavity and R the intensity reflectivity of both the input and output mirrors. Note that the round-trip time of the feedback loop is considered to be much shorter than τ_0 so that the feedback signal delay is neglected.

Equations (1)–(3) admit a spatially homogeneous steady-state solution $u_0=K[1-\cos(2\pi I_d)]$ and $I_d=I_0\equiv|A_0|^2$. Linear stability analysis of these equations gives the characteristic equation

$$\lambda=-(1+Dq^2)+2K\sin(2\pi I_0)(2\pi I_0)\sin(q^2L/2k_0), \tag{4}$$

where q is the wave number of the perturbation. $\lambda=0$ marks a Turing bifurcation, from which point the homogeneous steady state loses its stability, giving rise to static pattern formation. λ is cyclic in both the intensity I_0 and the square of the wave number q. This gives a two-dimensional array of instability islands in the (I_0,q^2) space. Figure 2(a) shows the first four instability domains in this space, for different values of $K=-0.05\pi$ and -0.1π, and fixed $D=0$. In general, the sizes of the islands increase with I_0 and $|K|$. For simplicity of analysis, we have in this work introduced a spatial frequency filter with a frequency cutoff of $q_{\mathrm{cut}}=\sqrt{2k_0\pi/L}$ before the feedback signal I_d is coupled to the phase modulator. The interactions between different instability islands in the q direction have therefore not been taken into account. For this case, instability in the steady-state solution u_0 occurs only in the areas where $\partial u/\partial I_0>0$ and its range increases with increase of I_0 until the full region is covered, as shown in Fig. 2(b).

Our numerical work focuses on the unstable region in the first cycle of $u_0(I_0)$. Three different domain pattern formations have been observed in this region on variation of the field intensity I_0. The numerical simulations are performed on a transverse square space with grid points $N=256$ and a size of some 18 times the characteristic length of the patterns. In the middle area of the unstable region stripe domain patterns emerge in both the phase and intensity of the light wave; the latter is shown in Fig. 3(a). Evolving from small-noise initial conditions, such a pattern is static after a transient period and is formed by patches of stripes. The stripes within each patch have a fixed but arbitrary orientation and almost constant wavelength, as confirmed by inspecting the power spectra of the signal, showing bright spots in a thin ring structure. The patches are shown to be mediated by various forms of defects, such as grain boundaries, dislocations, and disclinations, and mimic those observed in magnetic materials and Rayleigh-Bénard convection. On increasing I_0, dark spots emerge in the areas of these defects, from which small patches of π hexagon structure are formed in

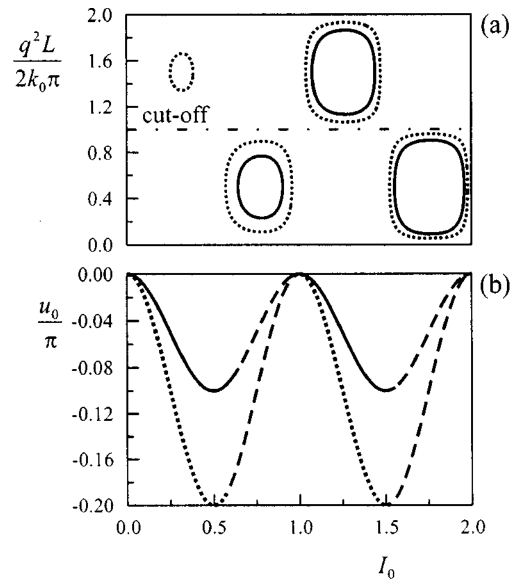

FIG. 2. (a) Instability islands in the bifurcation diagrams and (b) steady-state homogeneous solutions and their stabilities after the frequency cutoff from q_{cut} for two cases of different values of $K=-0.05\pi$ and -0.1π, depicted by solid and dotted lines, respectively. Dashed lines in (b) stand for unstable regions. D is fixed at $D=0$ for both cases.

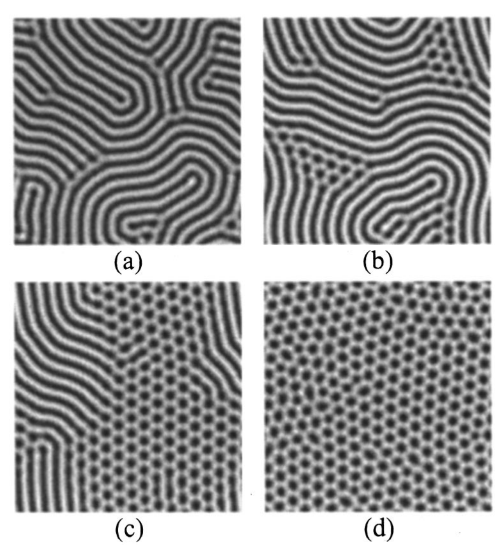

FIG. 3. Intensity distributions I_d for $K=-0.05\pi$, $D=0$, and different incident field intensities: (a) $I_0=0.781$, (b) $I_0=0.812$, (c) $I_0=0.817$, and (d) $I_0=0.844$, showing transitions of different domain pattern formations.

some regions where sufficient number of spots are formed, as shown in Fig. 3(b). The orientations of the hexagons are determined by the original alignment of the defects. The patterns are now dynamical. The competition of different structures results in slow drifting of the domains and their expansion and contraction in size in the transverse space. On further increasing I_0, the sizes of the hexagon patches increase through the emergence of more dark spots from the destabilized stripes, a snapshot of the coexisting stripe and hexagon domains being shown in Fig. 3(c). When I_0 is increased from this value, the hexagon patches seem to win the competition against stripes; their sizes increase and become dominant. As I_0 approaches the second Turing bifurcation point on the right side, pure hexagon domain patterns appear. They comprise patches of π hexagon structure with arbitrary orientations but the same wavelength. The patterns become static again. The connections of different domains are organized again through defects, such as pentagons and heptagons on the domain boundaries, as shown in Fig. 3(d). We note that the patterns on decreasing I_0 from the middle show similar features to those on increasing I_0, undergoing transitions from stripe domains to coexisting stripe and hexagon structures to hexagon domain patterns. The only difference for increasing I_0 is that the hexagons are 0 hexagons. Throughout this work we ran the simulation typically for a time of $50\,000\tau_0$, some ten times the transient period of the system, to determine whether patterns were static or dynamic.

The competition and transition of different domain patterns as demonstrated in the simulations may be understood from the stripe-hexagon interactions of our system. To this end we derive the amplitude equations for these basic pattern formations. For the case of small values of K the equations to third order [11] are sufficient to describe the evolution of the amplitude functions. They are given by

$$\tau_0\frac{dA_i}{dt}=\mu A_i+\eta A_j^*A_k^*-[\zeta_1|A_i|^2+\zeta_2(|A_j|^2+|A_k|^2)]A_i, \tag{5}$$

where $i,j,k=1,2,3$, and obey the convention of circular permutation. The four coefficients are relatively simple in our system and are given by

$$\mu=2K\sin(2\pi I_0)(2\pi I_0)-1,$$

$$\eta=2K[\sin(2\pi I_0)(2\pi I_0)+2\cos(2\pi I_0)(2\pi I_0)^2],$$

$$\zeta_1=4K[\sin(2\pi I_0)(2\pi I_0)+\sin(2\pi I_0)(2\pi I_0)^3],$$

$$\zeta_2=4K[\sin(2\pi I_0)(2\pi I_0)-2\cos(2\pi I_0)(2\pi I_0)^2 + 2\sin(2\pi I_0)(2\pi I_0)^3].$$

The stripes, given by $A_1=\sqrt{\mu/\zeta_1}\exp[i\varphi_1]$, $A_2=A_3=0$, and any circular permutation, are stable for $\mu>\eta^2\zeta_1/(\zeta_1-\zeta_2)^2>0$. Hexagon solutions are $A_{1,2,3}=H\exp[i\varphi_{1,2,3}]$, with $H_{1,2}^0=[\eta\pm\sqrt{\eta^2+4\mu(\zeta_1+2\zeta_2)}]/2(\zeta_1+2\zeta_2)$ for $\varphi_1+\varphi_2+\varphi_3=0$ and $H_{1,2}^\pi=[-\eta\pm\sqrt{\eta^2+4\mu(\zeta_1+2\zeta_2)}]/2(\zeta_1+2\zeta_2)$ for $\varphi_1+\varphi_2+\varphi_3=\pi$, corresponding to 0 and π hexagons respectively. The upper branches H_1^0 ($\eta>0$) and H_1^π ($\eta<0$) are stable for $-\eta^2/4(\zeta_1+2\zeta_2)<\mu<\eta^2(2\zeta_1+\zeta_2)/(\zeta_1-\zeta_2)^2$. The lower branches for both hexagon structures are always unstable. The amplitudes of stripe and hexagon solutions as functions of I_0 together with their stability are shown in Fig. 4. As seen, stripes are stable in the middle area against noise perturbations while 0 and π hexagons are stable on the left and right wings, respectively. In between there are two regions where both stripes and hexagons are stable. In these regions we have performed a further stability analysis of one solution against the other. It shows a small area of costable stripes and hexagons in each of the regions. We find that the stability regions of the three different patterns identified above by the amplitude equations correspond to the three different domain structures that we have observed numerically, namely, labyrinths, hexagon domain patterns, and coexisting stripe and hexagon domain structures.

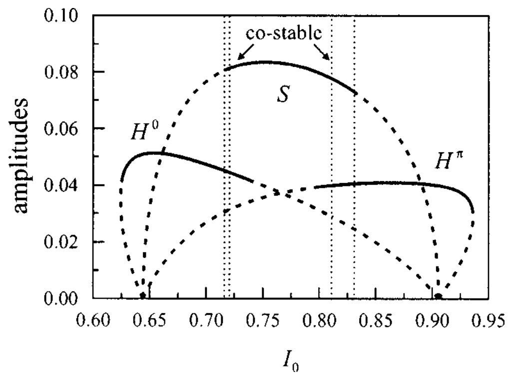

FIG. 4. Stationary-amplitude solutions of Eqs. (5) for $K=-0.05\pi$ and $D=0$. The solid (dashed) lines correspond to solutions stable (unstable) against noise perturbation. The areas between vertical dotted lines mark the two costable regions of stripes and hexagons. S, H^0, and H^π stand for stripes, 0 hexagons, and π hexagons, respectively.

While the parameter regions of the three different domain structures from our simulations can be identified using the amplitude equations, the existence of labyrinthine patterns, instead of straight stripes, cannot be explained by these simplified equations. Let us therefore investigate other types of pattern formation that may exist in this system. Figure 5 shows the bifurcation diagram in (I_0,K) space. There are two additional parameter regions identified to the left of the spontaneous pattern-forming area (SP), in which patterns are observed under hard excitations of the linearly stable homogeneous steady state. The leftmost curve marks the threshold for the emergence of localized states (LS's) with a circular-symmetric pulse excitation. The localized states have the usual Gaussian distribution with an oscillating tail when the two parameters K and I_0 are set in the area close to the threshold. However, away from the threshold curve, other forms of localized solution, such as a ring and a dot with a ring, are found to exist, as shown in the left inset of Fig. 5. In fact, when the incident light intensity is set close to the SP boundary, these different localized structures are multistable solutions of the system, which one appears depending on the initial condition of excitation. In general, more complicated structures usually correspond to higher strengths of initial

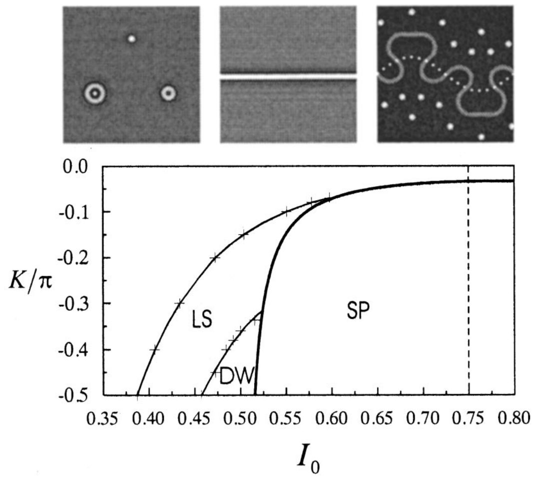

FIG. 5. Bifurcation diagram in (I_0,K) space shows three different pattern-forming regions. LS, DW, and SP correspond to localized states, domain walls, and spontaneous pattern. Localized states (left inset) are obtained for $K=-0.5\pi$, $I_0=0.512$, and $D=0$, for different strengths of initial excitation. Domain walls with localized states (right inset) are obtained using the same parameters but the initial excitation as the dashed line. Straight stripes can form in most of the DW region, using a straight or slightly curved stripe as initial condition.

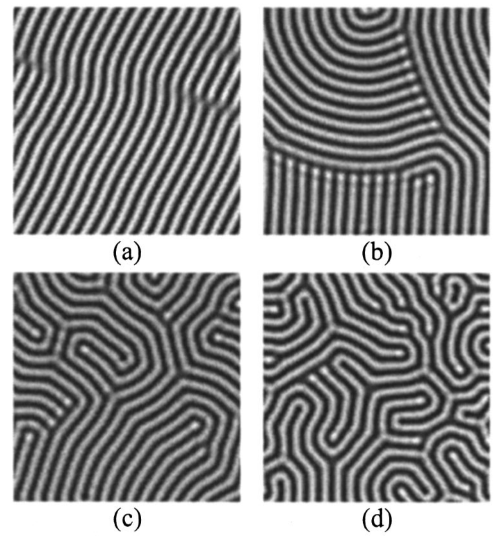

FIG. 6. Transition from ordered stripes to labyrinthine domain patterns on increasing K. The other parameters are set as $I_0=0.75$ and $D=0$.

excitation. Moreover, within the LS domain and close to the SP boundary, domain walls may form, the area of which is marked by DW. For instance, a straight stripe is stable, evolving from initial excitation of a straight or modestly zigzag-modulated stripe (Fig. 5, middle inset). This simulation result under periodic boundary conditions implies that such a straight stripe of infinite length is a solution of the system. We note that this stripe is static and therefore distinct from traveling-wave-front solutions in excitable reaction-diffusion systems [12]. More generally, we observe coexisting domain walls with localized states in this region using, for instance, more complicated curving stripes as initial conditions. In this case the localized states are created from evolving stripes during the transient period. The resulting patterns are static, an example being shown in the right inset of Fig. 5. The spots and walls in such a structure are shown to interact through their oscillating tails.

The existence of both domain walls and localized states is shown to extend to the SP region, though they are masked in this region by the spontaneous patterns, i.e., stripes and hexagons, as discussed earlier, and consequently the threshold for their appearance is difficult to identify clearly. It is the coexistence of and interaction between the hard excitation and spontaneous patterns that give rise to labyrinths and other domain patterns in this region. This can be clearly seen by investigating pattern evolution on increasing the feedback strength K (to the more negative direction) and with a fixed incident intensity, say $I_0=0.75$, corresponding to the vertical dashed line in Fig. 5. When K just enters the SP region, straight stripes emerge under weak noise perturbations to the homogeneous steady-state solution, the wavelength of which equals that at the critical point. On increasing K, curving stripes appear first with isolated dislocations [Fig. 6(a)] as more unstable wave numbers join the pattern selection process due to the growth of the instability island, as discussed earlier. On further increasing K, domain walls form and divide the pattern into domains of stripes with different orientations [Fig. 6(b)]. The domains become smaller and their numbers grow as the value of K increases [Figs. 6(c) and 6(d)]. The coefficient K is therefore an order parameter that can describe the coarsening process in this system. This provides the mechanism for development of the labyrinths from ordered patterns in our system. The scenario can also explain the existence of hexagon domains of different orientations as shown in Fig. 3, since the spontaneous pattern for that parameter set is the hexagon. We note that this mechanism is similar to that suggested in a degenerate optical parametric oscillator [13], in which labyrinths were considered as intermediate between patterns with defects and striped domain walls. Labyrinths have also been observed in an optical resonator with vectorial Kerr medium in which such patterns emerge as the system coarsens and domains grow [14].

We note that Fig. 5 shows only the left part of the pattern-forming region as presented in Fig. 4. The results are somewhat symmetrical between the left and right parts, if you take into account the dark (instead of bright) spots and walls on the right. Moreover, if the system operates in the next cycle with higher incident intensity [Fig. 2(b)], more complicated localized structures, domain stripes, and their coexistence have been observed, which are attributable to stronger phase modulations in the nonlinear medium due to increased incident light intensity in this region. Consequently, domains of complex forms of stripes appear in this parameter region.

Most useful discussions with Dr. M. A. Vorontsov and Professor R. G. Harrison are gratefully acknowledged. This work was supported by EPSRC (U.K.) Grant No. GR/M32573 and SHEFC (Scotland) Grant No. RDG/078.

[1] M. Seul, L. R. Monar, L. O'Gorman, and R. Wolfe, Science **254**, 1616 (1991).
[2] M. Seul and R. Wolfe, Phys. Rev. Lett. **68**, 2460 (1992).
[3] M. Seul, L. R. Monar, and L. O'Gorman, Philos. Mag. B **66**, 471 (1992).
[4] P. Coullet, T. Frisch, and G. Sonnino, Phys. Rev. E **49**, 2087 (1994); P. Coullet and K. Emilsson, Physica D **61**, 119 (1992).
[5] M. C. Cross and D. I. Meiron, Phys. Rev. Lett. **75**, 2152 (1995).
[6] R. E. Goldstein, D. J. Muraki, and D. M. Petrich, Phys. Rev. E **53**, 3933 (1996), and references therein.
[7] C. Bowman *et al.*, Physica D **123**, 474 (1999).
[8] C. Bowman and A. C. Newell, Rev. Mod. Phys. **70**, 289 (1998).
[9] M. A. Vorontsov, Yu. D. Dumarevsky, D. V. Pruidze, and V. I. Shmalhauzen, Izv. Akad. Nauk SSSR, Ser. Fiz. **52**, 374 (1988); S. A. Akhmanov, M. A. Vorontsov, and V. Yu. Ivanov, Pis'ma Zh. Eksp. Teor. Fiz. **77**, 611 (1988) [JETP Lett. **47**, 707 (1988)].
[10] M. A. Vorontsov, G. W. Carhart, and R. Dou, J. Opt. Soc. Am. B **17**, 266 (2000).
[11] S. Ciliberto *et al.*, Phys. Rev. Lett. **65**, 2370 (1990).
[12] W. Lu, D. Yu, and R. G. Harrison, Opt. Lett. **24**, 578 (1999), and references therein.
[13] M. Le Berre *et al.*, J. Opt. B: Quantum Semiclass. Opt. **2**, 347 (2000).
[14] R. Gallego *et al.*, Phys. Rev. E **61**, 2241 (2000).